Int. J. Heat Mass Transfer. Vol. 34, No. 8, pp. 2167–2173, 1991
Printed in Great Britain

0017-9310/91 $3.00+0.00
Pergamon Press plc

Low Prandtl number convection in a rectangular cavity with longitudinal thermal gradient and transverse *g*-jitters

DIDIER THEVENARD
CEA/DTA/CEREM/DEM, Section d'Etudes de la Solidification et de la Cristallogenèse, 85X, 38041 Grenoble Cedex, France

and

HAMDA BEN HADID
Institut de Mécanique des Fluides, CNRS-LA03, 1 rue Honnorat, 13003 Marseille, France

(*Received* 15 *June* 1989 *and in final form* 19 *November* 1990)

1. INTRODUCTION

MATERIALS processing in space, such as crystal growth, may be sometimes disturbed by residual accelerations, or *g*-jitters, which act on the space carrier: atmospheric drag, gravity gradient effect, vibrations, crew activities, etc. Because of the presence of thermal gradients (and thus of density gradients) in the liquid phase of the experiment these residual accelerations may give rise to convective motions; in turn, these convective flows may act on the solute field and lead to heterogeneities of dopant in the grown crystal. Thus it is important to be able to predict the possible influence of *g*-jitters on solidification experiments, and to forecast whether or not they may lead to a lower quality of space-grown crystals.

With this aim, this note will be devoted to *g*-jitter convection in an ideal crystal growth configuration. A second paper (to be published) will be devoted to the influence of *g*-jitter convection on the distribution of solute (or dopant) in the liquid phase. Here we shall assume that the liquid alloy is dilute enough to enable a separate computation of velocity and solute fields (no solutal convection). The crystal growth experiment is modelled by a *bidimensional*, rectangular cavity (Fig. 1), with end walls held at temperatures $T_0-\Delta T/2$ and $T_0+\Delta T/2$, and totally filled with a Newtonian, low Prandtl number liquid at mean temperature T_0; side walls are adiabatic and all surfaces are rigid no-slip boundaries. We shall study convective flows induced by *g*-jitters transverse to the thermal gradient; we chose this orientation of the *g*-jitters because it is the most 'critical', i.e. there is no threshold for the onset of convection as there would be in a 'Rayleigh–Bénard' configuration. The pioneering work in this field is that of Dressler [1], who studied the response of the system to a step of gravity. Our method will be somewhat different from his. We shall consider the effect of a single fluctuation of gravity, defined as

$$\mathbf{g} = \mathbf{g}\, e^{2i\pi ft}$$

with f the frequency of the *g*-jitter and $i^2 = -1$ (we use complex notations for periodic phenomena). We look for non-dimensional velocities and streamfunctions in the form

$$\mathbf{v} = \mathbf{v}(x,y)\, e^{2i\pi\tau}, \quad \psi = \psi(x,y)\, e^{2i\pi\tau}$$

where $\mathbf{v}(x, y)$ and $\psi(x, y)$ are *complex* to take possible *phase shifts* between the gravity fluctuation and the flow into account. The non-dimensional equations of the problem are therefore

$$\nabla\cdot\mathbf{v} = 0 \tag{1}$$

$$\nabla \wedge (2i\pi\, Fq\, \mathbf{v} - \nabla^2\mathbf{v} - Gr\, x\mathbf{j}) = 0 \tag{2}$$

with the boundary conditions

$$\mathbf{v} = 0 \quad \text{at} \quad x = \pm Az/2,\ y = \pm 1/2. \tag{3}$$

The symbols in equations (1)–(3) are defined in the Nomenclature; Gr is the classical Grashof number based on the gradient and Fq a non-dimensional frequency. We assumed that the fluid is Boussinesq-incompressible and we neglected, as it is usual to do for low Grashof numbers, the $(\mathbf{v}\cdot\nabla)\mathbf{v}$ term in front of $\nabla^2\mathbf{v}$ in equation (2). Another approximation lies in the assumption, valid for low-Prandtl-number fluids, that the longitudinal temperature field in the cavity is nearly diffusive, consequently leading in the $Gr\,x$ term in equation (2).

Setting $\mathbf{v} = \nabla \wedge \psi$ we also obtain the streamfunction formulation of the problem

$$2i\pi\, Fq\, \nabla^2\psi = \nabla^4\psi - Gr \tag{4}$$

with the boundary conditions

$$\psi = \frac{\partial\psi}{\partial x} = \frac{\partial\psi}{\partial y} = 0 \quad \text{for} \quad x = \pm Az/2,\ y = \pm 1/2. \tag{5}$$

We first give an exact analytical solution of this problem in the case of an infinite cavity (Section 2.1), and approximate this solution to the case of a rectangular cavity of finite length (Section 2.2). Then we compare this solution with numerical (time-dependent, finite difference) computations (Section 3). In the last part of this work we shall briefly show how to extend the previous results to cylindrical configurations and how to calculate the response of the fluid to a superimposition of several mono-frequency *g*-jitters.

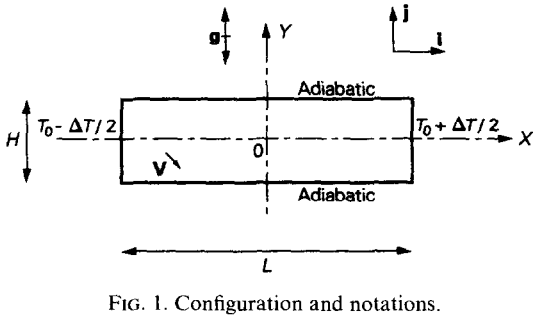

FIG. 1. Configuration and notations.

NOMENCLATURE

f	frequency of the g-jitter
g	gravity level or amplitude of the g-jitter (ground : g_0)
$\mathbf{g}$	gravity vector
$\mathscr{G}$	thermal gradient, $\Delta T/L$
H	height of the cavity
i	complex number, $\sqrt{-1}$
$\mathbf{i}, \mathbf{j}$	reference vectors (see Fig. 1)
L	length of the cavity
t	time
T_0	average temperature in the liquid
ΔT	temperature difference between the ends of the cavity
$\mathbf{V}$	velocity vector of the fluid
$\mathbf{v}$	non-dimensional velocity vector
X, Y	coordinates
x, y	non-dimensional coordinates.

Greek symbols

α	thermal diffusivity coefficient of the liquid
β	coefficient of thermal expansion of the liquid
ν	kinematic viscosity of the liquid
τ	non-dimensional time
ψ	streamfunction.

Non-dimensional parameters

Az	aspect ratio of the cavity, L/H
Fq	non-dimensional frequency, fH^2/ν
Gr	Grashof number based on the gradient, $g\beta\mathscr{G}H^4/\nu^2$
Pr	Prandtl number, ν/α
Re	Reynolds number : maximum of $\lvert\mathbf{v}\rvert$.

Miscellaneous symbols

∇	Nabla operator, $(\partial/\partial x, \partial/\partial y)$
$\wedge$	dot product.

2. ANALYTICAL SOLUTIONS

2.1. *g-Jitter convection in an infinite cavity*

If we let $Az \to +\infty$ in equations (1)–(3) and if we hold meanwhile the thermal gradient constant, the problem becomes that of a bidimensional, infinite layer of fluid subject to a constant longitudinal thermal gradient and to a fluctuating gravity $\mathbf{g}$ normal to the layer. The reader can easily check that *there is no solution with* $\mathbf{v} = 0$: the layer of fluid cannot stay at rest. This is the reason why the gravity perturbations transverse to the thermal gradient are always very critical, since the slightest fluctuation of the gravity is able to put the fluid into motion (no 'threshold'). The solution in the steady state is well known and given by Birikh's [2] or Hart's [3] formula

$$\mathbf{v} = \begin{cases} \frac{1}{6}Gr\, y(y-\frac{1}{2})(y+\frac{1}{2}) \\ 0 \end{cases}. \tag{6}$$

The corresponding streamfunction is given straightforwardly by an integration

$$\psi = \frac{Gr}{24}(y-\tfrac{1}{2})^2(y+\tfrac{1}{2})^2. \tag{7}$$

In the case of a fluctuating gravity the solution is also quite easy to find

$$\mathbf{v} = \begin{cases} \dfrac{1}{4\pi}\dfrac{Gr}{Fq}\mathbf{i}\left(2y - \dfrac{\sinh(\sqrt{(2\pi\mathrm{i}\,Fq)}y)}{\sinh(\sqrt{(2\pi\mathrm{i}\,Fq)}/2)}\right) \\ 0 \end{cases} \tag{8}$$

or when using the streamfunction

$$\psi = \frac{1}{4\pi}\frac{Gr}{Fq}\mathrm{i}h(y) \tag{9}$$

where h is a complex function defined as

$$h(z) = \left(z^2 - \frac{1}{\sqrt{(2\pi\mathrm{i}\,Fq)}}\right. \times \left.\frac{\cosh(\sqrt{(2\pi\mathrm{i}\,Fq)}z) - \cosh(\sqrt{(2\pi\mathrm{i}\,Fq)}/2)}{\sinh(\sqrt{(2\pi\mathrm{i}\,Fq)}/2)} - \frac{1}{4}\right). \tag{10}$$

2.1.1. *Analysis of the velocity fields in an infinite cavity.* The above solution shows some characteristic and noteworthy features that we shall outline below.

(1) *Maximum velocity.* Figure 2(a) shows the maximum velocity, as given by equation (8), as a function of the frequency of the g-jitter (with non-dimensional numbers: the Reynolds number Re as a function of Fq). For the low values of Fq, the maximum velocity is nearby the one found for the steady convection (see equation (6), Birikh/Hart profile). For the high values of Fq, the velocity decreases and behaves like $1/Fq$; this result was already mentioned by several authors, including Monti *et al.* [4]; Griffin and Motakef mention a similar result in a 'vertical' configuration [5]. The transition occurs near $\log(Fq) = 0.8$, that is, $Fq \simeq 6$.

(2) *Velocity profile.* Figure 2(b) gives the profile of the velocity field inside the cavity, $\lvert\mathbf{v}\rvert$ divided by its maximum value, for various values of the frequency. At low frequencies the profile is similar to Birikh's one (see Fig. 6). For $Fq \gg 10$ the maximum of the profile comes closer to the walls of the cavity. Without making any rigorous demonstration, this fact may be explained as follows: let $Fq \to +\infty$ in equation (4)

$$2\mathrm{i}\pi\, Fq\, \nabla^2\psi = \nabla^4\psi - Gr \tag{4}$$

then ψ tends towards the solution of

$$2\mathrm{i}\pi\, Fq\, \nabla^2\psi = -Gr \tag{11}$$

because $\lvert\psi_{\max}\rvert$ behaves like $1/Fq$ and thus the $\nabla^4\psi$ term becomes 'negligible' in front of the other terms. The solution of equation (11) with the boundary conditions $\psi = 0$ for $y = \pm 1/2$ is

$$\psi_{\text{asympto}} = \frac{\mathrm{i}}{4\pi}\frac{Gr}{Fq}(y^2 - \tfrac{1}{4}) \tag{12}$$

or in terms of velocity

$$\mathbf{v}_{\text{asympto}} = \begin{cases} \dfrac{\mathrm{i}}{2\pi}\dfrac{Gr}{Fq}y \\ 0 \end{cases}. \tag{13}$$

But two orders of derivation are lost between equations (4) and (11); so two boundary conditions must be lost, that is the two conditions

$$\frac{\partial\psi}{\partial y} = 0 \quad \text{for} \quad y = \pm 1/2 \tag{14}$$

which are not fulfilled by the asymptotic solution (12). Thus there must be a 'boundary layer' which matches the asymptotic solution with the boundary condition (14) near $y = \pm 1/2$. This is what Fig. 2(b) shows: when $Fq \to +\infty$, the velocity profile tends towards the linear profile defined by equation (13) except near the walls where the profile is coupled with the no-slip condition at the walls.

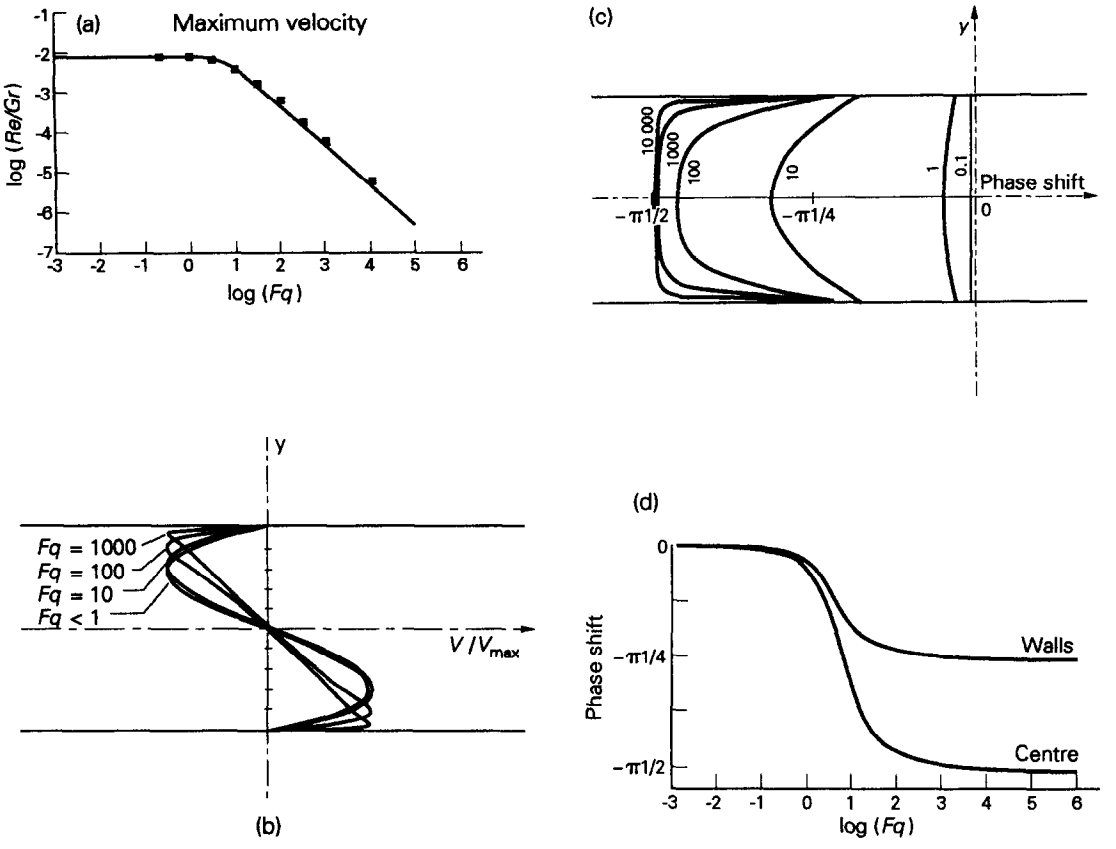

FIG. 2. Velocity field in a cavity of infinite length, for various values of the non-dimensional frequency Fq: (a) maximum velocity in the cavity vs Fq; (b) velocity profile in the cavity, for Fq ranging from 1 to 1000; (c) phase shift between gravity and fluid velocity, for Fq ranging from 1 to 10000; (d) phase shift on the walls and at the centre of the cavity vs Fq.

(3) *Phase shift.* Figure 2(c) shows the phase shift between ψ and the excitation $g\,e^{2i\pi ft}$, as a function of the position y in the cavity and of the non-dimensional frequency Fq. For low frequencies, the fluid 'follows' the fluctuation of the gravity, in phase; at high frequencies the centre of the fluid layer responds with a lag of $-\pi/2$. This is not surprising since this was also shown by the asymptotic solution (13); it means that the fluid phase behaves like a dynamic system with low damping. The phase shift is always maximum in the centre of the cavity and minimum at the walls; it tends towards $-\pi/4$ at the walls for high frequencies. Figure 2(d) shows the evolution of minimum/maximum phase shifts as a function of frequency.

2.2. *g-Jitter convection in a rectangular cavity*

The case of the rectangular cavity is a little bit more difficult. The main reason is that there is no exact analytical solution to the simplified system (1)–(3) or (4) and (5), even in the steady case. An approximate solution at $Fq = 0$ is given by Batchelor's formula [6]

$$\psi = \frac{2}{3}\frac{Az^4}{1+Az^4}Gr\left(\frac{x}{Az}-\frac{1}{2}\right)^2\left(\frac{x}{Az}+\frac{1}{2}\right)^2\left(y-\frac{1}{2}\right)^2\left(y+\frac{1}{2}\right)^2. \tag{15}$$

The corresponding velocity profile is cubic for both y and x, and is antisymmetrical with respect to the centre of the cavity.

Please note that Batchelor's solution is *not* exact. Batchelor in his article refers to Love, *A Treatise on the Mathematical Theory of Elasticity* (Cambridge University Press, 1927), Chap. 22, who explains that the solution

"... was given long ago by Grashof... the formula, *though devoid of theoretical foundation*, has often been treated with respect".

The exact solution may be calculated by an infinite series, the coefficients of which are themselves solutions of an infinite system of equations. The fact that Batchelor's solution has no theoretical justification should not be considered as critical. This solution agrees quite well with more precise computations for a square cavity and describes with reasonable agreement the flows for aspect ratios up to 2; and at last, $\psi(0, y)$ tends towards the *exact* solution of Birikh when Az becomes infinite. Therefore, we shall use Batchelor's formulae hereafter for aspect ratios (Az) up to 2. In the case of the fluctuating gravity we shall look for an *approximate* solution similar to Batchelor's one, and therefore assume the following hypotheses:

(1) ψ may be written as $\psi(x, y) = \phi(x/Az)\cdot\phi(y)$;

(2) when the frequency tends towards 0, ψ should tend towards Batchelor's solution;

(3) when the aspect ratio becomes infinite, $\psi(0, y)$ should tend towards the 'infinite cavity' solution of Section 3.1.

Hypothesis (1) is reasonable, first because equation (4) is symmetrical in x and y, and also because the approximate

solution in the steady state (Batchelor's solution) also shares this feature. Hypothesis (2) is really obvious and hypothesis (3) is also a reasonable condition, which is also fulfilled by Batchelor's solution.

Hypotheses (1)–(3) lead directly to the form of ψ

$$\psi(x,y) = \frac{1}{4\pi}\frac{Gr}{Fq}\,\mathrm{i}\,\frac{Az^4}{(1+Az^4)}\,\frac{h(x/Az)h(y)}{h(0)} \qquad (16)$$

where h is the function defined before (formula (10))

$$h(z) = \left(z^2 - \frac{1}{\sqrt{(2\pi\mathrm{i}\,Fq)}} \times \frac{\cosh(\sqrt{(2\pi\mathrm{i}\,Fq)}z) - \cosh(\sqrt{(2\pi\mathrm{i}\,Fq)}/2)}{\sinh(\sqrt{(2\pi\mathrm{i}\,Fq)}/2)} - \frac{1}{4}\right).$$

This solution is thought to be valid in the same conditions as Batchelor's one, i.e. for aspect ratios up to 2. The properties of ψ proceed from those studied in Section 2.1 for the infinite cavity. For low frequencies ($Fq \to 0$) we find Batchelor's solution again (by hypothesis) and no phase shift between ψ and $g\,\mathrm{e}^{2\mathrm{i}\pi t}$. At high frequencies ($Fq \to +\infty$) ψ tends towards

$$\psi_{\text{asympto}} = \frac{1}{4\pi}\frac{Gr}{Fq}\,\mathrm{i}\,\frac{Az^4}{(1+Az^4)}\left(\frac{x^2}{Az^2} - \frac{1}{4}\right)\left(y^2 - \frac{1}{4}\right)$$

which means a linear velocity profile, except near the walls (boundary layer, as before). The phase shift between ψ and g is 0 in the corners of the cavity and is maximum in the centre. It tends towards $-\pi/2$ in the centre when the frequency becomes infinite and towards $-\pi/4$ at the centre of the walls.

2.3. *The extended rectangular cavity with fluctuating gravity*

We still have to pay attention to the case between the infinite cavity (Section 2.1) and the rectangular cavity of aspect ratio less than 2 (Section 2.2). A paper by Cormack *et al.* is devoted to this problem in the case of steady convection [7]. They suggest to study separately the flow in the centre of the cavity, represented by a streamfunction ψ_{core}, and the flow in the ends, ψ_{end}, with an asymptotic matching condition. They find that the matching between both solutions occurs at a distance 1 from the ends, that is, *the spatial extent on which the ends have an influence is equal to the height of the cavity*. This suggests a very simple (though not completely correct) way to calculate the flows in cavities of aspect ratio greater than 2. The cavity is divided into a central region, where the flow is described by the streamfunction (9), and two end regions where the flow is described by formulae like (16), written for half cavities of aspect ratio 2 centred at $x = Az/2 - 1$ and $-Az/2 + 1$. The matching of both solutions occurs obviously at a distance 1 from the ends. We shall see an example of this in the next section where we compare the analytical formulae with a numerical computation in the case of a cavity of aspect ratio 4.

3. NUMERICAL STUDY

A numerical study of the basic equations (with low but non-zero Prandtl number and without neglecting the quadratic term in equation (2)) was performed, in order to check the accuracy of the analytical solutions of the previous section. A cavity of aspect ratio 4 was chosen for the numerical computations. This aspect ratio is a good compromise; it is not too long, so big meshes and computing cost are avoided, but it is long enough to enable two kinds of flows to coexist: a *core flow* similar to the flow in an infinite cavity, and an *end flow* near the ends. Thus each calculation gives a maximum of information.

3.1. *Description of the numerical method*

Here we shall give an overview of the numerical method used. The governing equations are now expressed in vorticity–streamfunction formulation. Then the equations are discretized by using a time-and-space finite difference scheme based on an ADI (alternating direction implicit) technique.

For space derivatives, we used a Hermitian method in which the variables and their first and second derivatives are taken as unknowns. The Hermitian relations used to close the system are those given in ref. [8] and obtained from a Taylor series expansion. This results in a 3×3 block-tridiagonal system which is solved with an efficient Thomas algorithm. To solve the vorticity equation, the requested values of the wall vorticity are obtained by explicit evaluation of the streamfunction equation at the wall, by considering a Hermitian relation of fourth-order accuracy

$$\zeta_w = \left(\frac{\partial^2\psi}{\partial\mathbf{n}^2}\right)_w = -\frac{1}{2h^2}[7\psi_{w+2} + 16\psi_{w+1} - 23\psi_w] + \frac{1}{h}\left[\left(\frac{\partial\psi}{\partial\mathbf{n}}\right)_{w+2} + 8\left(\frac{\partial\psi}{\partial\mathbf{n}}\right)_{w+1} - 6\left(\frac{\partial\psi}{\partial\mathbf{n}}\right)_w\right]$$

where ψ is the streamfunction, ζ the vorticity and $\mathbf{n}$ the normal to the boundary. For a stiff problem the algorithm involves internal iterations at two levels. The first one concerns the streamfunction equation and the second the boundary conditions for the vorticity transport equation. For more information about the technique used the reader can refer to refs. [9, 10]. A variable 81×21 grid generated by the Thompson method [11] was used with grid points much more clustered near the walls to better see the displacement of the velocity profile at high frequencies. The Prandtl number for all computations was set equal to 0.015 (liquid tin) and the Grashof number to $Gr = 10$. All the computations were performed on a Cray 2 computer.

Two kinds of problems were encountered:

(1) The numerical scheme is stable only if the time step remains lower than a given value (which depends on the space step). This turned out to be problematic at *low frequencies*, because the number of time steps necessary to go through a period of the g-jitter becomes too important.

(2) The computations were carried out by decreasing frequencies: the starting state of the computation for a given frequency was the final state of the computation for the previous frequency. The problem with such a method is that there is a transient regime at the beginning of the computation: at *high frequencies*, the number of iterations to reach the permanent regime was too long. When we started the numerical work we did not know the analytical solutions (9) and (16). A better way to speed up the computation would have been to take these solutions as starting points for the computations.

Finally flows were computed for the following non-dimensional frequencies: $Fq = 0.2, 1, 3.33, 10, 33.3, 100, 333, 1000, 10\,000$.

3.2. *Main results*

(1) *Maximum velocity*. The maximum velocity is reached in the 'core' region of the cavity. Numerical results were superimposed on Fig. 2(a). The points are very close to the analytical values found for an infinite cavity.

(2) *Velocity profile*. Figure 3 gives the evolution of the velocity profiles on the medians of the cavity, as a function of frequency. They are compared with the profiles defined in Section 2.2.

(a) In the *core region* of the cavity, the profiles are nearly exactly those we found analytically in the case of the infinite cavity. The little shift observed at $Fq = 10^3$ is probably attributable to numerical problems (the computation is carried out near the limit of precision of the program).

(b) Near the *ends* of the cavity the agreement is not so good. This was expected: the analytical solution, even for the steady state, is just an approximation. Nevertheless and qualitatively speaking, both results show the same charac-

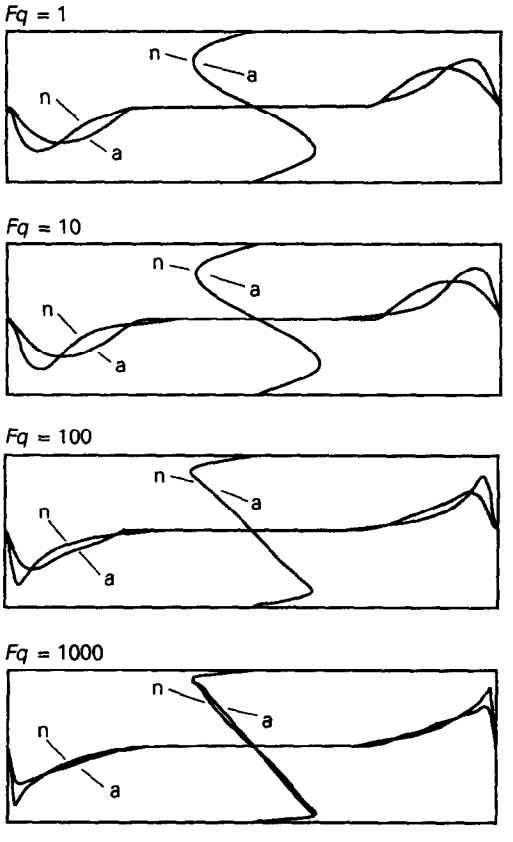

FIG. 3. Velocity profiles on the medians of a cavity of aspect ratio $Az = 4$, for frequencies ranging from 1 to 1000. Analytical results (a) and numerical results (n).

teristic features: displacement of the velocity profile near the walls at high frequencies, spatial extent of the end effects.

(3) *Phase shifts.* The analysis of the phase shifts gives rise to several difficulties. First it is very sensitive to numerical errors; afterwards, the limited number of iterations per step (about ten) does not enable a good accuracy on the phase shift; at last, for obvious reasons, it is not possible to compute the phase shift on the walls, where the velocity is equal to zero. Nevertheless, a reasonable agreement was found between analytical and numerical solutions. More specifically, the increase of the phase shift with frequency was observed, with its $-\pi/2$ limit in the centre of the cavity and its $-\pi/4$ limit on the medians.

3.3. *Conclusions*

The analytical formulae seem to give a reasonably good description of the flow in a rectangular cavity with longitudinal thermal gradient and transverse g-jitters. In the central part of extended cavities ($Az \gg 1$) the flow is described nearly exactly by the 'infinite cavity' solution. End effects are perceptible up to a distance 1 from the ends, and analytical formulae give a good idea of the recirculation in the end regions. There is little effect of the aspect ratio except for $Az < 2$. The same kind of solution may be used for the recirculation in the ends of extended cavities and for the flow in short ($Az < 2$) cavities. At last the behaviour of the fluid at very high frequencies is very interesting; except near the walls, the flow may be described by asymptotic expressions with a $-\pi/2$ phase shift.

The good agreement between numerical results and analytical formulae is a very encouraging point for a wide use of these formulae. For example, they may be used to get a first idea on the sensitivity of a given space experiment to residual accelerations. This is especially true for crystal growth experiments, for which the aspect ratio varies with time: the calculus is quite easy with the analytical formulae, whereas it would require a considerable amount of computer hours to get the corresponding numerical solutions. On the other hand, these analytical formulae may be very helpful in numerical works, as they may be used as starting solutions to speed up the convergence of numerical computations.

4. DISCUSSION

The extension of the solutions obtained for bidimensional, rectangular cavities to the case of cylindrical cavities may in some cases give rise to some problems. The flows in a bidimensional cavity and in the middle plane of a cylindrical cavity are often said to be similar; as long as the Grashof number is not too high this is legitimate, but does not give indications on the flow in other parts of the cavity. Tridimensional effects may possibly occur, especially near the ends. Beside this fact, bidimensional models seem to overestimate by one third the velocities inside cylindrical enclosures. On all these topics see the synthesis article by Bontoux *et al.* [12].

To finish with it may be interesting to extend the results obtained in the case of a mono-frequency disturbance to 'real' situations were several frequencies (and possibly an infinity of frequencies) add up. Equations (1)–(3) show a *linear* relation between the fluctuations of gravity and the velocity fields inside the cavity. Therefore, when gravity sums up several frequencies, we should expect that the velocity field inside the cavity to be the sum of all the velocity fields calculated separately for all frequencies. It must be stressed that this is true only if the hypotheses that led to the linear system (1)–(3) remain fulfilled: low Prandtl number, low Rayleigh number (and thus low Grashof number). More specifically the conclusions about g-jitter convection have to be revised if the fluid is not a liquid metal, for example water or gas, or if the Grashof number is too high (greater than 2000, for example). Please remember that the Grashof number varies like the fourth power of the cavity's height; for the growth of 'industrial' crystals (2″, 3″) in microgravity, the Grashof number may rapidly become too high to let the previous analysis be still valid.

A practical application of this study is shown on Fig. 4. We consider here the space solidification of a ∅ 1″ Ge(Ga) crystal, with a thermal gradient, e.g. 50 K cm^{-1}; the aspect ratio will be set equal to 4. The parameters of the experiment are summarized in Table 1.

The spectrum of the residual gravity considered here is shown on Fig. 4(a). It has an 'infinity' of frequencies (in fact 512, to enable the use of a Fast Fourier Transform algorithm) with a low-frequency characteristic component at 1.85×10^{-4} Hz corresponding to the orbital period of the host spacecraft, about 90 min. This situation may be encountered aboard spacecraft like EURECA, which keep a constant orientation with respect to the sun and thus 'rotates' in a geocentric system of coordinates: the orientation of the residual gravity varies along the orbit with a period equal to the time of revolution. Figure 4(b) gives, as a function of time, the evolution of the velocity at point $(0, -1/2\sqrt{3})$, i.e.

Table 1

H	height	cm	2.54
α	thermal diffusivity	cm^2 s^{-1}	0.21
β	thermal expansion coefficient	K^{-1}	9.4E−05
ν	kinematic viscosity	cm^2 s^{-1}	1.4E−03
$\mathscr{G}$	thermal gradient	K cm^{-1}	50

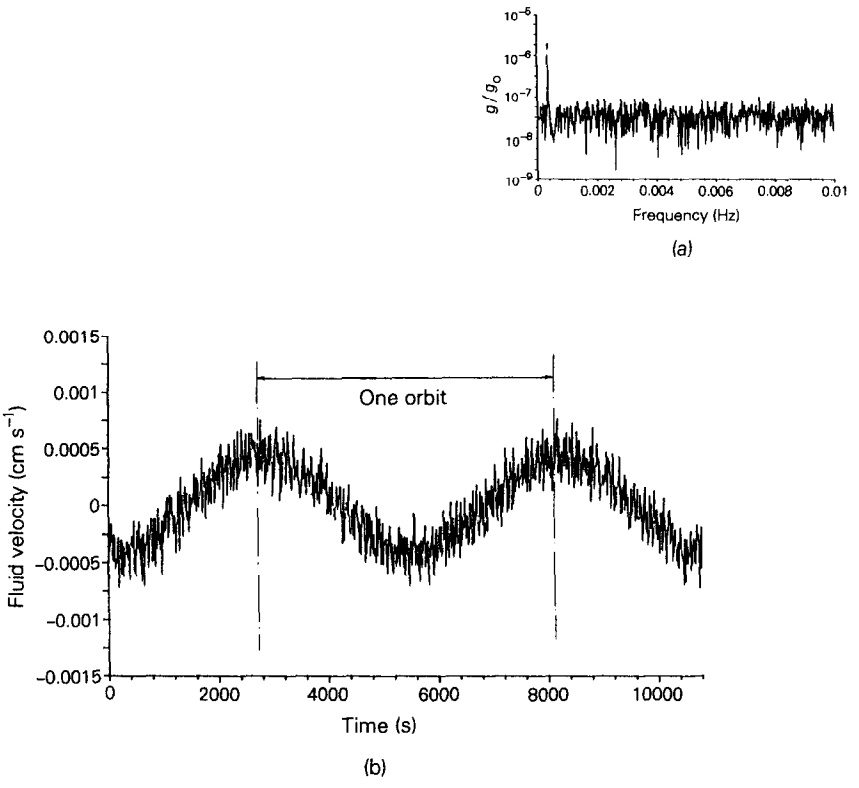

FIG. 4. Test case: (a) gravity spectrum, with a low-frequency component at $10^{-6}g_0$; (b) response of the fluid.

where the steady component of the velocity is maximum. The calculus is achieved through formula (8) for each single frequency and an inverse Fourier transform is used to switch back to the time domain. It is clear on Fig. 4(b) that the fluid 'follows' the characteristic low-frequency fluctuation of the residual gravity along the orbit, whereas higher frequencies are damped. This is in good agreement with what we already know: as shown on Fig. 2(a) the fluid behaves like a first-order system, with a cut-off frequency at $Fq \simeq 6$ or dimensionally: $f = 1.3\text{E}-03$ Hz. Thus, mainly those frequencies lower than that value will have a direct impact on the experiment.

A second paper, to be published [13], will be devoted to the alterations of the solute field induced by the motion of the liquid during a crystal growth experiment. It will be shown whether the velocities, though very low (here some 10^{-4} cm s^{-1}) are liable or not to have an influence on crystal growth processes.

Acknowledgements—This work was supported by the European Space Agency under contract 7681/88. One of us (D. Thevenard) is partly supported by AEROSPATIALE, Division Systèmes Stratégiques et Spatiaux, and wishes to express numerous thanks to this company for having made possible his participation in the study. The computations were carried out on the Cray 2 of the C.C.V.R. (Centre de Calcul Vectoriel pour la Recherche) using IBM facilities of the C.N.U.S.C. (Centre National Universitaire Sud de Calcul). The present work was conducted within the GRAMME agreement between CEA–IRF and CNES.

REFERENCES

1. R. F. Dressler, Transient thermal convection during orbit spaceflight, *J. Crystal Growth* **54**, 523–533 (1981).
2. R. V. Birikh, Thermocapillary convection in a horizontal layer of liquid, *J. Appl. Mech. Tech. Phys.* **3**, 69–72 (1966).
3. J. E. Hart, Low Prandtl number convection between differentially heated end walls, *Int. J. Heat Mass Transfer* **2**, 1069–1074 (1983).
4. R. Monti, D. Langbein and J. J. Favier, Influence of residual acceleration on fluid physics and materials science experiments. In *Fluid Sciences and Material Sciences in Space* (Edited by H. U. Walter), Chap. XVIII, pp. 637–680. ESA publication, Springer, Berlin (1987).
5. P. R. Griffin and S. Motakef, Analysis of the fluid dynamics and heat transfer during micro-gravity Bridgman–Stockbarger growth of semiconductors in steady periodic gravitational fields, ASME Paper 87-WA/HT-1, presented at the ASME Winter Annual Meeting, Boston, Massachusetts, 13–18 December (1987).
6. G. K. Batchelor, Heat transfer by free convection across a closed cavity between vertical boundaries at different temperatures, *Q. Appl. Math.* **XII**(3), 209–233 (1954).
7. D. E. Cormack, L. G. Leal and J. H. Imberger, Natural convection in a shallow cavity with differentially heated end walls, Part 1: asymptotic theory, *J. Fluid Mech.* **65**, 209–229 (1974).
8. T. E. Hirsh, Higher order accurate difference solutions of fluid mechanics problems by a compact differencing technique, *J. Comput. Phys.* **19**, 90–109 (1975).
9. H. Ben Hadid and B. Roux, Steady and unsteady flow regimes in shallow cavities filled with low-Prandtl num-

ber fluids. In *Notes on Numerical Fluid Mechanics*. Ed. Vieweg (1989).
10. H. Ben Hadid, Thèse de Doctorat d'Etat, Université d'Aix-Marseille II, France (1989).
11. P. Thompson, K. H. Thames and J. E. Mastin, Automatic numerical generation of a body-fitted curvilinear coordinate system, *J. Comput. Phys.* **15,** 299–319 (1974).
12. P. Bontoux, B. Roux, G. H. Schiroky, B. L. Markham and F. Rosenberger, Convection in the vertical midplane of a horizontal cylinder, comparison of two-dimensional approximations with three-dimensional results, *Int. J. Heat Mass Transfer* **29,** 227–240 (1986).
13. D. Thevenard and J. J. Favier, Influence of g-jitters on the solidification of dilute alloys, *Proc. VIIth European Symp. on Materials and Fluid Sciences in Space*, Oxford, U.K., 10–15 September (1989).